JCI The Journal of Clinical Investigation

IL-15 protects NKT cells from inhibition by tumor-associated macrophages and enhances antimetastatic activity

Daofeng Liu, … , Gianpietro Dotti, Leonid S. Metelitsa

J Clin Invest. 2012;122(6):2221-2233. https://doi.org/10.1172/JCI59535.

Research Article **Oncology**

Vα24-invariant NKT cells inhibit tumor growth by targeting tumor-associated macrophages (TAMs). Tumor progression therefore requires that TAMs evade NKT cell activity through yet-unknown mechanisms. Here we report that a subset of cells in neuroblastoma (NB) cell lines and primary tumors expresses membrane-bound TNF-α (mbTNF-α). These proinflammatory tumor cells induced production of the chemokine CCL20 from TAMs via activation of the NF-κB signaling pathway, an effect that was amplified in hypoxia. Flow cytometry analyses of human primary NB tumors revealed selective accumulation of CCL20 in TAMs. Neutralization of the chemokine inhibited in vitro migration of NKT cells toward tumor-conditioned hypoxic monocytes and localization of NKT cells to NB grafts in mice. We also found that hypoxia impaired NKT cell viability and function. Thus, CCL20-producing TAMs served as a hypoxic trap for tumor-infiltrating NKT cells. IL-15 protected antigen-activated NKT cells from hypoxia, and transgenic expression of IL-15 in adoptively transferred NKT cells dramatically enhanced their antimetastatic activity in mice. Thus, tumor-induced chemokine production in hypoxic TAMs and consequent chemoattraction and inhibition of NKT cells represents a mechanism of immune escape that can be reversed by adoptive immunotherapy with IL-15–transduced NKT cells.

IL-15 protects NKT cells from inhibition by tumor-associated macrophages and enhances antimetastatic activity

Daofeng Liu,[1] Liping Song,[1] Jie Wei,[1] Amy N. Courtney,[1] Xiuhua Gao,[1] Ekaterina Marinova,[1] Linjie Guo,[1] Andras Heczey,[1] Shahab Asgharzadeh,[2] Eugene Kim,[1] Gianpietro Dotti,[3] and Leonid S. Metelitsa[1,3]

[1]Department of Pediatrics and Department of Pathology and Immunology, Texas Children's Cancer Center, Baylor College of Medicine, Houston, Texas, USA. [2]Division of Hematology-Oncology, Department of Pediatrics, Childrens Hospital Los Angeles and Keck School of Medicine, University of Southern California, Los Angeles, California, USA. [3]Center for Cell and Gene Therapy, Baylor College of Medicine, Houston, Texas, USA.

Vα24-invariant NKT cells inhibit tumor growth by targeting tumor-associated macrophages (TAMs). Tumor progression therefore requires that TAMs evade NKT cell activity through yet-unknown mechanisms. Here we report that a subset of cells in neuroblastoma (NB) cell lines and primary tumors expresses membrane-bound TNF-α (mbTNF-α). These proinflammatory tumor cells induced production of the chemokine CCL20 from TAMs via activation of the NF-κB signaling pathway, an effect that was amplified in hypoxia. Flow cytometry analyses of human primary NB tumors revealed selective accumulation of CCL20 in TAMs. Neutralization of the chemokine inhibited in vitro migration of NKT cells toward tumor-conditioned hypoxic monocytes and localization of NKT cells to NB grafts in mice. We also found that hypoxia impaired NKT cell viability and function. Thus, CCL20-producing TAMs served as a hypoxic trap for tumor-infiltrating NKT cells. IL-15 protected antigen-activated NKT cells from hypoxia, and transgenic expression of IL-15 in adoptively transferred NKT cells dramatically enhanced their antimetastatic activity in mice. Thus, tumor-induced chemokine production in hypoxic TAMs and consequent chemoattraction and inhibition of NKT cells represents a mechanism of immune escape that can be reversed by adoptive immunotherapy with IL-15–transduced NKT cells.

Introduction

Vα24-invariant NKT cells are an evolutionary conserved sublineage of T cells that are characterized by the expression of an invariant TCR α-chain, Vα24-Jα18, and reactivity to self- and microbial-derived glycolipids presented by the monomorphic HLA class I–like molecule CD1d (1). The antitumor potential of NKT cells has been demonstrated in numerous tumor models (2–4). Selective decreases in number and/or functional activity of NKT cells have been reported in patients with diverse types of cancer (5–7), which suggests that NKT cells may play an important role in the antitumor immune responses and, conversely, that an escape from NKT cells may contribute to tumor progression. Our group previously demonstrated that NKT cells infiltrate primary human tumors in a subset of children with neuroblastoma (NB) and that NKT cell infiltration is associated with improved long-term disease-free survival (8). NKT cell infiltration in primary tumors also served as a prognostic factor of favorable outcome in patients with colorectal cancers (9), while low levels of circulating NKT cells predicted a poor clinical outcome in patients with head and neck squamous cell carcinoma (10).

Because the majority of solid tumors are $CD1d^-$, tumor cells cannot be a direct target for NKT cell cytotoxicity (3, 11). Instead, tumor-associated macrophages (TAMs) are the only cells in primary NB tumors that have detectable CD1d expression (12). Moreover, upon recognition of tumor-derived glycolipids, NKT cells produce IFN-γ and kill monocytic cells in a CD1d-dependent manner. Since TAMs provide a critical stromal support for tumor cell growth in NB and many other types of cancer (13–15), NKT cell–mediated killing or inhibition of TAMs explains how NKT cells may indirectly impede tumor growth. Other recent reports have generated additional evidence for the importance of NKT cell interactions with monocytic cells and other myeloid cells in viral and tumor immunity (16, 17) and in the potential mechanism of antitumor activity of the NKT cell ligand β-manosylceramide (18).

Monocytes and other immature myelomonocytic precursors of TAMs localize to the tumor site in response to CCL2, the same chemokine that attracts NKT cells (8). Monocytic cells, however, respond to multiple other tumor-derived chemotactic signals that are not recognized by NKT or other T cells (19). The majority of these factors (e.g., VEGF, endothelin, and angiopoietin-2) are produced in hypoxic conditions and drive TAM migration to the hypoxic areas (13, 19, 20). Importantly, hypoxic signaling amplifies NF-κB activation in TAMs, leading to high levels of IL-6 production and sustained STAT3 activation in tumor cells that in turn promote inflammatory responses in TAMs, providing a positive feedback loop that plays an essential role in tumor progression (21).

Although NKT cells colocalize with IL-6–producing TAMs in primary NB tissues (12), the mechanism of this colocalization is not understood, nor is it clear how TAMs evade the inhibitory activities of NKT cells. An understanding of the NKT-TAM interaction in the context of tumor microenvironment is critically important for the development of rational cancer immunotherapy that targets tumor-supportive stroma, given that NKT cells are the only known immune effector cells that specifically recognize and negatively regulate TAMs. Here, we demonstrated that NKT cell localization to NB depended not only on tumor-derived CCL2,

Conflict of interest: The authors have declared that no conflict of interest exists.
Citation for this article: *J Clin Invest.* 2012;122(6):2221–2233. doi:10.1172/JCI59535.

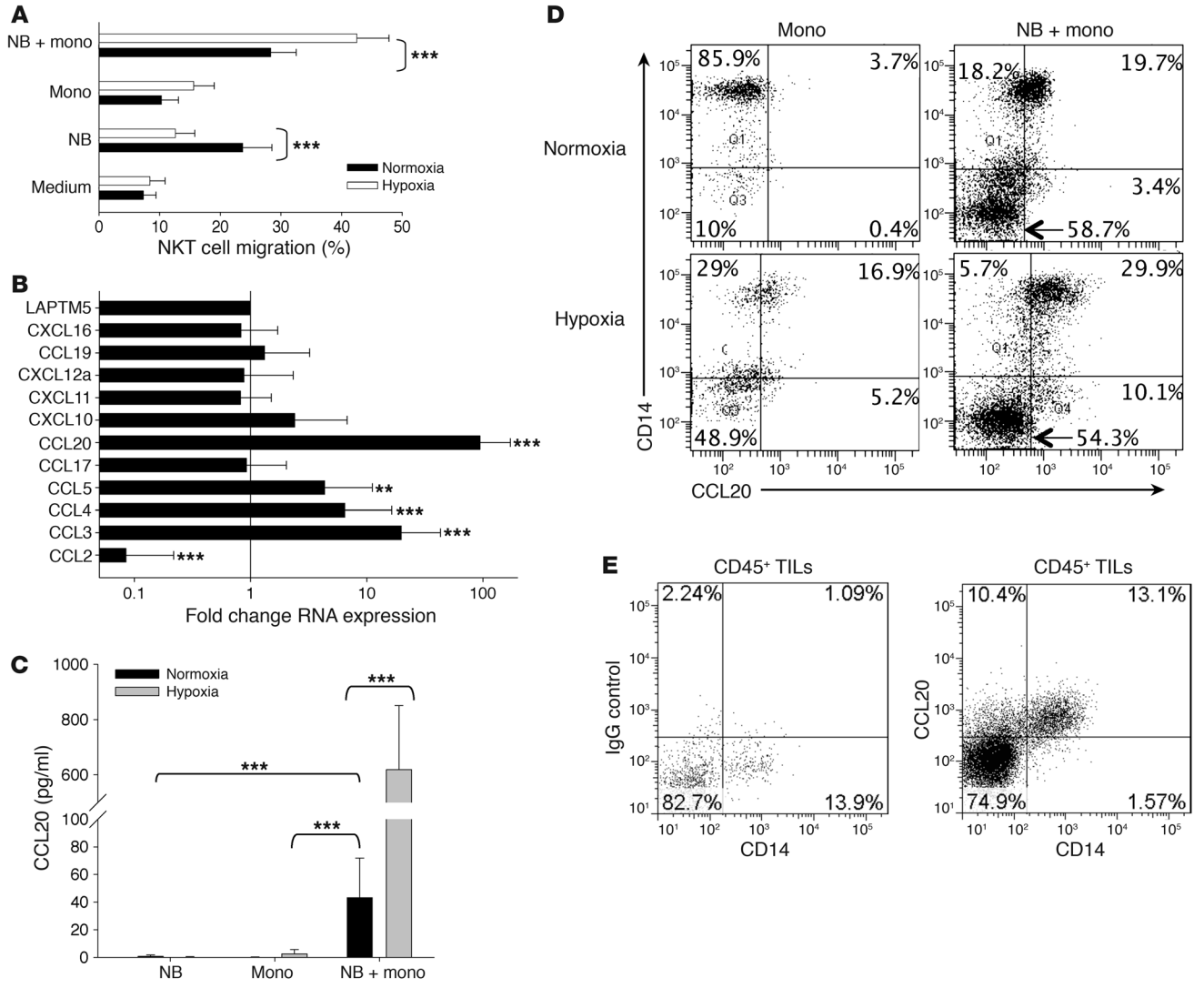

Figure 1

Contact with NB cells and hypoxia synergistically induce CCL20 in human monocytes. (**A**) Primary monocytes were cocultured with CHLA-255 NB cells (1:1 ratio) for 48 hours in normoxic (20% O_2) or hypoxic (1% O_2) conditions, and supernatants were placed in bottom chambers of dual-chambers plates with 5-μM pore membranes with or without addition of the indicated neutralizing antibodies or their isotype control. NKT cells were placed in the upper chambers and allowed to migrate for 3 hours, and the rate of NKT cell migration was quantified by FACS. Results are mean ± SD from 3 experiments in triplicate. (**B**) Monocytes were cocultured with or without CHLA-255 NB cells for 36 hours in normoxic or hypoxic conditions followed by mRNA isolation and quantitative real-time PCR analysis of 11 chemokine genes known to attract human NKT cells. Data are from a representative of 3 experiments in triplicate. (**C**) Monocytes and CHLA-255 NB cells were cultured alone or combined in hypoxic or normoxic conditions for 48 hours. CCL20 concentration was quantified in the supernatants using ELISA. Data are mean ± SD from experiments with monocytes from 6 donors in duplicate. (**D**) Cells were cultured as in **C** and analyzed for intracellular CCL20 accumulation in $CD14^+$ monocytes and $CD14^-$ NB cells. Regions were set using corresponding isotype controls. Data are from a representative of 3 experiments in duplicate. (**E**) Tumor-infiltrating leukocytes (TILs) were isolated from a cell suspension of freshly resected primary NB by gradient centrifugation and cultured with GolgiStop for 4 hours followed by FACS. After gating on $CD45^+$ events, CCL20 accumulation was examined in $CD14^+$ TAMs and compared with the corresponding isotype control. Data are from a representative of 3 experiments. $^{**}P < 0.01$; $^{***}P < 0.001$.

but also on CCL20, which was produced by TAMs in response to tumor-induced inflammation and hypoxia and in turn inhibited NKT cell viability and function. We also showed that IL-15 protected antigen-activated NKT cells from hypoxia and that transgenic expression of IL-15 in NKT cells strongly enhanced their antitumor efficacy in a metastatic NB model in humanized NOD/SCID/IL-2Rγ–null (hu-NSG) mice.

Results

Contact with NB cells and hypoxia synergistically induce CCL20 in human monocytes. To explain the observed colocalization of NKT cells with TAMs in primary human NB (12), we hypothesized that TAMs upon the influence of tumor cells and/or hypoxic environment actively chemoattract NKT cells. To test this hypothesis, we performed an in vitro migration experiment using dual-chamber wells

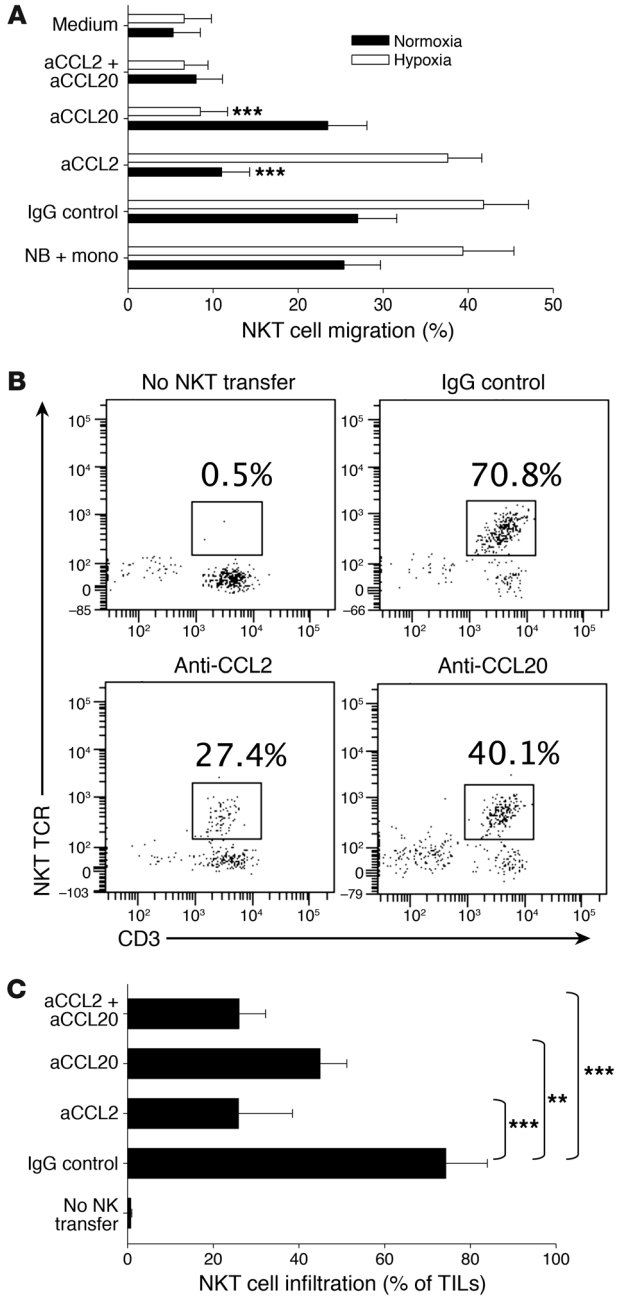

Figure 2
CCL20 is required for NKT cell migration toward hypoxic NB and monocyte culture and NB tumors in hu-NSG mice. (**A**) Monocytes were cocultured with CHLA-255 NB cells for 48 hours in normoxic or hypoxic conditions, followed by analysis of NKT cell in vitro migration with or without neutralizing antibodies (a-) or their isotype control, as in Figure 1A. Results are mean ± SD from 3 experiments in triplicate. (**B**) Xenografts of CHLA-255/luc cells were established under renal capsule of hu-NSG mice followed by i.v. transfer of ex vivo–expanded human NKT cells (5×10^7 per mouse) or PBS (control). Just before NKT cell transfer, mice received i.p. injections of neutralizing antibodies or their isotype control. The tumor-infiltrating leukocytes were analyzed by FACS on day 3 after NKT cell transfer. After gating on $hCD45^+$ cells, NKT cells were identified as $CD3^+Va24\text{-}Ja18^+$ events. Data are from a representative of 5 mice per group. (**C**) Tumor-infiltrating NKT cell frequency (mean ± SD) from **B**. $^{**}P < 0.01$; $^{***}P < 0.001$.

separated by 5-μM pore membrane. Human ex vivo–expanded NKT cells were added to the upper chambers and allowed to migrate for 3 hours into the lower wells, which contained CHLA-255 NB cells, freshly isolated (negative selection) human monocytes from peripheral blood, or 1:1 mixture of NB cells and monocytes. Before adding NKT cells, the plates with NB cells and monocytes were incubated in normoxic (20% O_2) or hypoxic (1% O_2) conditions for 48 hours. Consistent with our previous observations, NB cells were chemoattractive for NKT cells in normoxic conditions (8). Surprisingly, NKT cell migration to NB cells was nearly abrogated in hypoxia ($P < 0.001$; Figure 1A). In contrast, the rate of NKT cell migration toward the coculture of NB cells with monocytes nearly doubled under hypoxic conditions ($P < 0.001$), whereas monocytes alone had little chemoattractive activity in either normoxia or hypoxia. These data suggest that an interaction between NB cells and monocytes under hypoxia results in induction (upregulation) of chemokines that chemoattract NKT cells.

To examine the overall effect of hypoxia on the chemokine gene expression profile of NB cells and monocytes, we incubated monocytes and CHLA-255 NB cells in normoxic or hypoxic conditions for 36 hours followed by RNA isolation and quantitative RT-PCR for 11 CC and CXC chemokine genes that are known to have corresponding receptors on human NKT cells (8, 22–25). mRNA expression of CCL20, CCL5, CCL4, and CCL3 was upregulated, whereas that of CCL2 was downregulated, in hypoxia compared with normoxia ($P < 0.001$; Figure 1B). We previously reported that, unlike other chemokines, CCL2 is expressed at high levels in NB cells, and additional experiments with NB cells alone confirmed that hypoxia downregulated CCL2 expression in NB cells at both RNA and protein levels (data not shown). This finding explains the observed loss of NB cell chemoattraction for NKT cells in hypoxia. To examine whether the upregulation of mRNA expression of CCL20, CCL5, CCL4, and CCL3 results in increased production of the corresponding proteins, we analyzed supernatants from the same experimental conditions by ELISA. Only CCL20 production was significantly upregulated in the coculture of monocytes with NB cells compared with monocytes alone (NB cells do not produce detectable CCL20). Moreover, the effect of the coculture on CCL20 upregulation was amplified up to 70-fold in hypoxic compared with normoxic conditions ($P < 0.001$; Figure 1C and Supplemental Figure 1A; supplemental material available online with this article; doi:10.1172/JCI59535DS1). Despite the observed variability in the magnitude of CCL20 production by monocytes from 13 different individuals, hypoxia invariably increased it in all cases. The kinetics analysis demonstrated that upregulation of CCL20 reached maximum levels after 36 hours of coculture in normoxia, but continued to rise for at least 48 hours in hypoxia (Supplemental Figure 1B).

To unambiguously determine the cellular source of CCL20, we cultured monocytes alone or with NB cells in normoxic or hypoxic conditions and analyzed intracellular CCL20 accumulation by fluorescence-activated cell sorting (FACS) using surface staining for CD14 to discriminate monocytes from NB cells. Either contact with NB cells or hypoxia alone could upregulate CCL20 production in monocytes (Figure 1D). The highest level of CCL20 expression was achieved when monocytes were cocultured with

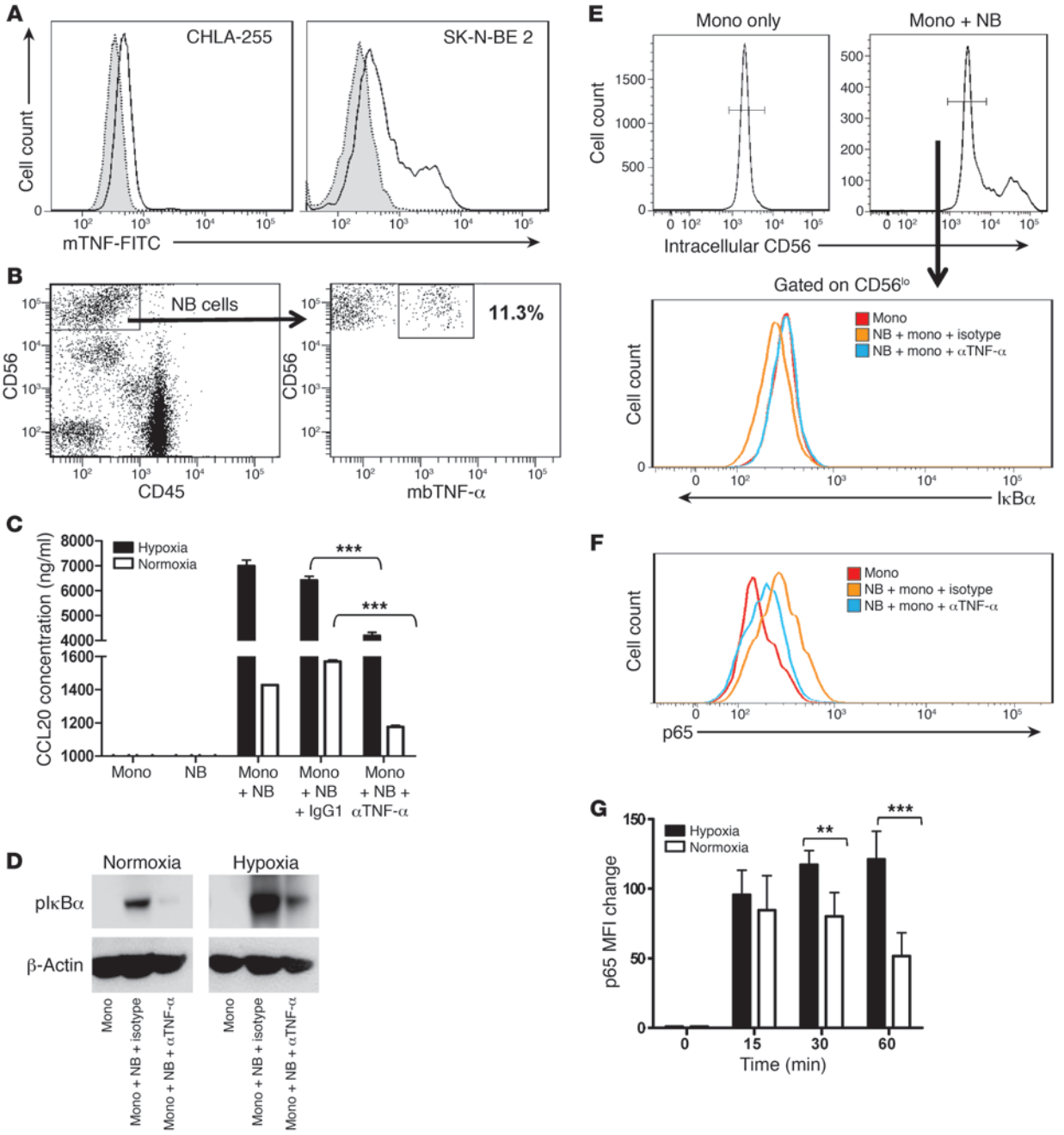

Figure 3

mbTNF-α on NB cells induces NF-κB activation in monocytes. (**A**) Cultured NB cells were suspended using 2% EDTA without trypsin and analyzed by FACS for cell surface expression of mbTNF-α in 2 representative NB cell lines (shaded, isotype control; open, anti–mbTNF-α). (**B**) Cell suspensions from freshly resected primary NB tumors were stained for surface markers. mbTNF-α expression on NB cells was analyzed after gating on $CD56^{hi}CD45^{-}$ events. (**C**) NB cells were preincubated with 50 ng/ml anti-human TNF-α or isotype control mAb for 1 hour before addition of monocytes; NB and monocytes alone were used as controls. CCL20 concentration in the culture supernatant was determined by ELISA after 36 hours. Results are mean ± SD from 3 experiments in triplicate. ***$P < 0.001$, 1-way ANOVA. (**D**) Monocytes were cultured alone in nonadherent plates or on top of NB cell monolayer, with addition of anti–TNF-α or isotype control mAb, in normoxia or hypoxia for 16 hours followed by monocyte detachment and Western blotting for phospho-IκBα using β-actin as a loading control. Data are from a representative of 3 experiments. (**E** and **F**) The same experiment as in **D** was followed by intracellular staining for (**E**) IκBα or (**F**) phospho-p65 in monocytes after gating out NB cells as $CD56^{hi}$ events. (**G**) Kinetics of phospho-p65 expression in monocytes upon coculture with NB cells in normoxic and hypoxic conditions. Results are mean ± SD from 2 experiments in triplicate. **$P < 0.01$; ***$P < 0.001$.

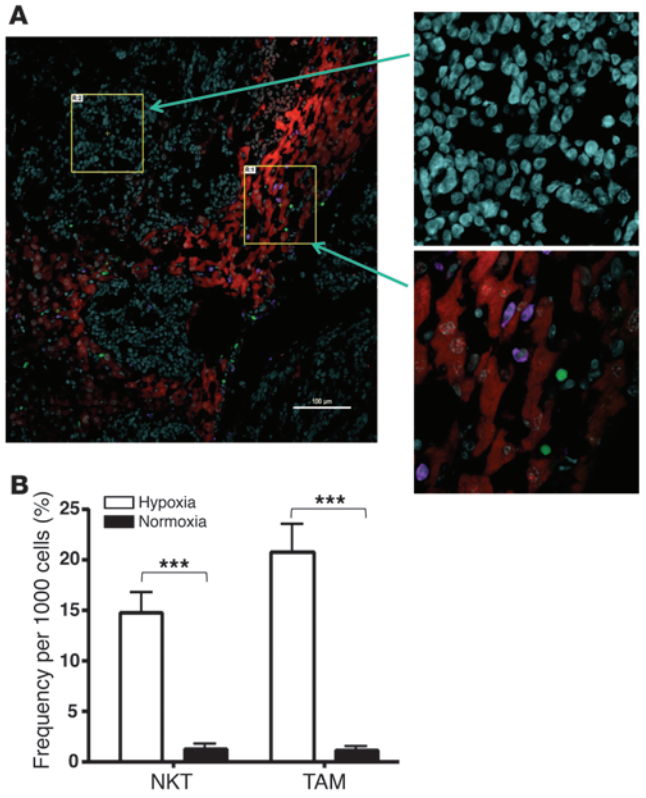

Figure 4
NKT cells preferentially localize to hypoxic areas within tumor tissues. At 3 months after SCT, hu-NSG mice (see Methods) received i.v. injection of 10^6 CHLA-255/luc NB cells; 3 weeks later, mice were injected with CFSE-labeled NKT cells. For labeling hypoxic tissues, mice were i.v. injected with EF5 3 hours before being euthanized. (**A**) Immunofluorescent analysis of liver metastasis for hypoxia (Cy3–anti-EF5; red), NKT cells (CFSE; green), and human myeloid cells (hCD11b; violet). Magnified images (left, ×20; right, ×60) show typical areas of normoxic and hypoxic tissues. Shown are representative of 10 100-μm fields analyzed per mouse, 5 mice per experiment, 2 independent experiments. Scale bar: 100 μm. (**B**) Image analysis (see Methods). Regions with mean Cy3 intensity lower than 200 and higher than 550 were defined as normoxic and hypoxic, respectively. Absolute numbers of NKT cells and hCD11b$^+$ cells in normoxic and hypoxic regions were counted in 10 100-μm fields per mouse, 5 mice per group. Shown are number of tumor-infiltrating NKT and CD11b$^+$ cells per 1,000 cells (mean ± SD) in 1 of 2 experiments with similar results. ***$P < 0.001$.

NB cells in hypoxia, consistent with the ELISA results in Figure 1C. NB cells did not express detectable CCL20 in any tested condition. To examine the requirement of cell-cell contact between monocytes and NB cells for CCL20 induction in monocytes, we cultured NB cells with monocytes in the same wells or in the dual-chamber wells, separated by a 400-nM semipermeable membrane. Monocytes failed to produce CCL20 in the absence of direct contact with NB cells (Supplemental Figure 1C). To determine whether the induction of CCL20 in monocytes that we observed in the described in vitro experimental system occurs at the tumor site in NB patients, we performed FACS on cell suspensions prepared from freshly resected primary NB tumors at diagnosis. We found that all tumor-derived monocytic cells expressed CCL20, whereas tumor cells and the majority of nonmonocytic CD45$^+$ tumor-infiltrating leukocytes were negative (Figure 1E). Therefore, TAMs in primary NB tumors produced CCL20, expression of which was selectively induced in monocytic cells upon direct contact with NB cells and enhanced by hypoxia.

CCL20 is required for NKT cell migration toward hypoxic NB-monocyte culture and NB xenografts in hu-NSG mice. CCL20 has been reported to be one of the most potent chemokines for human NKT cells (23, 24). Our analysis confirmed that the majority of primary NKT cells from peripheral blood expressed CCR6, the only receptor for CCL20. Moreover, CCR6 expression was preserved in ex vivo–expanded NKT cells (Supplemental Figure 2). To determine the requirement of the CCL20/CCR6 axis for the observed enhanced migration of NKT cells toward the coculture of NB cells with monocytes in hypoxia (Figure 1A), we repeated the in vitro migration experiment in the presence of chemokine-neutralizing mAbs. Consistent with our previous report (8), anti-CCL2 mAb effectively inhibited NKT cell migration to NB cells or NB-monocyte coculture under normoxia, but not under hypoxia. Only anti-CCL20 neutralizing mAb strongly inhibited NKT cell migration in hypoxia ($P < 0.001$; Figure 2A).

To examine the relative contribution of CCL2 and CCL20 to the mechanism of NKT cell in vivo localization to the tumor site, we adapted a previously described CHLA-255/luc human NB model in immunodeficient mice (12) and, instead of NOD/SCID, used hu-NSG mice (Supplemental Figure 3A). As has been observed by others (26, 27), hu-NSG mice had stable reconstitution of human myelomonocytic cells as well as B and T lymphocytes 3 months after stem cell transplantation (SCT) with human cord blood CD34$^+$ hematopoietic stem cells (Supplemental Figure 3, B and C). We injected CHLA-255/luc NB cells under the renal capsule 3.5 months after SCT. Like in human NB tissues (12), TAMs represented a major subset of tumor-infiltrating leukocytes (Supplemental Figure 3, D and E) and were enriched in a subset with M2 phenotype, as determined by the downregulation of HLA-DR expression compared with CD14$^+$ peripheral blood monocytes in the same mice (Supplemental Figure 3F). Importantly, similar HLA-DR^{lo}CD14$^+$ cells were the dominant subset of TAMs in primary tumors from NB patients (Supplemental Figure 3G). At 3 weeks after NB cell injection and clear evidence of tumor growth by bioluminescent imaging, mice were injected with human ex-vivo–expanded NKT cells and divided into groups to receive anti-human CCL2, anti-human CCL20 neutralizing mAb, both mAbs combined, or isotype control mAb. A control group did not receive NKT cells. On day 3 after NKT cell transfer, mice were euthanized and examined for NKT cell localization to the tumor tissues. Animals treated with anti-CCL2 or anti-CCL20 mAb had lower frequency of tumor-infiltrating NKT cells among the tumor-infiltrating human CD45$^+$ (hCD45$^+$) leukocytes (25.9% ± 12.6% and 44.9% ± 6.3%, respectively) compared with the

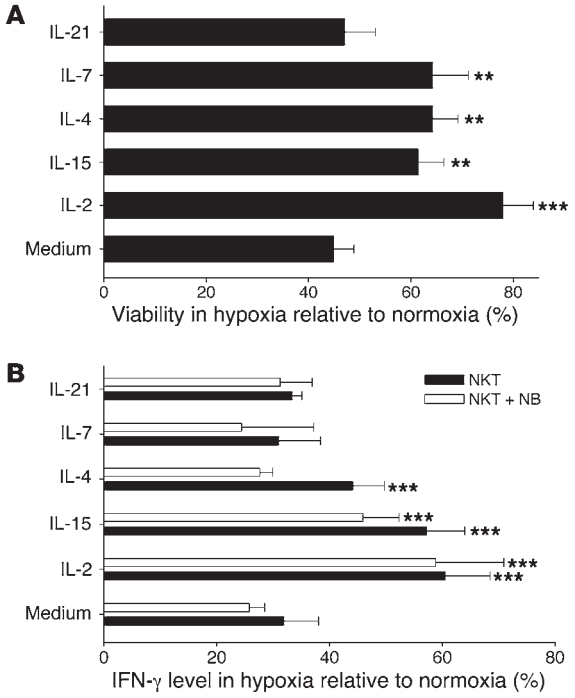

Figure 5
NKT cell viability and function are inhibited by hypoxia and protected by cytokines. (**A**) NKT cells were expanded from PBMCs of 4 donors using stimulation with αGalCer and cultured under hypoxia or normoxia in the presence or absence of the indicated cytokines at 200 U/ml for 24 hours. The number of viable cells was quantified using hemocytometer and trypan blue staining. (**B**) NKT cells were cultured for 24 hours as in **A**, followed by TCR stimulation with 6B11 mAb. Cytokine release was quantified by CBAPlex assay from 24-hour supernatants. The cytokine amount was normalized by percent viable cells in the corresponding conditions. Results are mean ± SD from 3 experiments in triplicate. $^{**}P < 0.01$; $^{***}P < 0.001$.

IgG control group (74.3% ± 9.7%, $P < 0.01$; Figure 2, B and C). The neutralization of both chemokines did not increase inhibition of NKT cell migration more than the neutralization of CCL2 alone (26% ± 6.2%, $P < 0.001$; Figure 2C), which suggests that the chemokines act along the same axis. While confirming the previously established role of NB-derived CCL2, these data also established the requirement of CCL20 for NKT cell localization to the tumor site, even though the latter chemokine was not produced by tumor cells, but induced in TAMs. Thus, NKT cells effectively localized to NB tumors in hu-NSG mice and migrated toward TAMs in a CCL20-dependent manner.

mbTNF-α on NB cells induces NF-κB activation in monocytes that results in CCL20 upregulation. The observed requirement for cell-cell contact between NB cells and monocytes for CCL20 induction in monocytes and the known requirement of NF-κB activation for CCL20 expression (28) prompted us to search for candidate cell surface molecules on NB cells with proinflammatory properties. Goillot et al. observed expression of TNF-α protein in 2 NB cell lines by immunohistochemistry (29). We here examined 3 MYCN-amplified (SK-N-BE2, IMR32, LA-N1) and 3 non–MYCN-amplified (CHLA-255, CHLA-15, LA-N-2) NB cell lines by FACS and found that the majority of cells in all lines expressed TNF-α intracellularly (Supplemental Figure 4), as well as on the cell surface as a membrane-bound cytokine (Figure 3A). No soluble TNF-α was detected by ELISA in the supernatants of all examined cell lines. Importantly, we found the presence of the membrane-bound TNF-α–positive (mbTNF-α^+) subset in all 7 examined primary NB tumors, with the frequency ranging from 1.1% to 38.2% (12.2% ± 14%; Figure 3B). The level of MYCN expression did not correlate with the frequency of mbTNF-α^+ cells, either in cell lines or in primary tumors (data not shown). The function blocking experiments demonstrated that preincubation of NB cells with an anti–TNF-α blocking mAb significantly inhibited their ability to induce CCL20 production in monocytes under both normoxic and hypoxic conditions ($P < 0.001$; Figure 3C). Neither the frequency of TNF-α^+ cells nor the level of TNF-α expression in NB cells was affected by hypoxia (data not shown). To examine the requirement of mbTNF-α for the activation of NF-κB signaling in monocytes, we cultured monocytes alone (in nonadherent plates) or on the monolayer of NB cells (because monocytes only loosely adhere to the NB cell monolayer) in the presence of an isotype control or anti–TNF-α blocking mAb in normoxic or hypoxic conditions. IκBα, an IκB inhibitor, was phosphorylated (a required upstream event in NF-κB activation by extracellular stimuli) in monocytes upon contact with NB cells, and the IκBα phosphorylation was almost completely prevented in the presence of anti–TNF-α blocking mAb (Figure 3D). The hypoxic condition enhanced IκBα phosphorylation, and this was also strongly inhibited by the anti–TNF-α blocking mAb. Since contaminating NB cells could not be excluded as a source of phospho-IκBα in the above-described monocyte preparations, we repeated this experiment and performed intracellular FACS analysis of IκBα and phosphorylated p65. After gating on $CD56^{lo}$ cells (monocytes), we observed a decrease of IκBα expression (degradation upon phosphorylation) within 30 minutes of contact with NB cells, and the effect was abrogated in the presence of anti–TNF-α blocking mAb (Figure 3E). Consistent with the decreased IκBα expression, we observed increased phospho-p65 expression in monocytes, and this was inhibited by anti–TNF-α blocking mAb in normoxic (Figure 3F) and hypoxic (data not shown) conditions. Coculture of monocytes with NB cells under hypoxia resulted in higher levels and more sustained p65 expression compared with normoxia ($P < 0.01$; Figure 3G). We conclude that NB contains a subset of proinflammatory tumor cells that express mbTNF-α, which is required at least in part for the induction of CCL20 production in TAMs via activation of NF-κB signaling, which is stabilized and enhanced by tumor-induced hypoxia.

NKT cells preferentially localize to hypoxic areas within tumor tissues. To examine the relative distribution of NKT cells in hypoxic and normoxic areas of the tumor, we used a metastatic model of NB in hu-NSG mice. In this model, CHLA-255/luc cells were injected i.v. to produce metastatic growth in liver and bone/bone marrow (see below), the major metastatic sites in NB patients (30). On day 21, tumor-bearing mice were injected with CFSE-labeled NKT cells, and their localization in liver metastases was examined 3 days later. The areas of hypoxia in both primary and metastatic sites were visualized using intravital injection of EF5 followed by staining with anti-EF5 fluorochrom-conjugated mAb (31). The same tissues were costained with anti-CD11b mAb, so that distribution of both NKT cells and myeloid cells in normoxic and hypoxic tumor tissues was analyzed and quantified using 4-color confocal microscopy. In con-

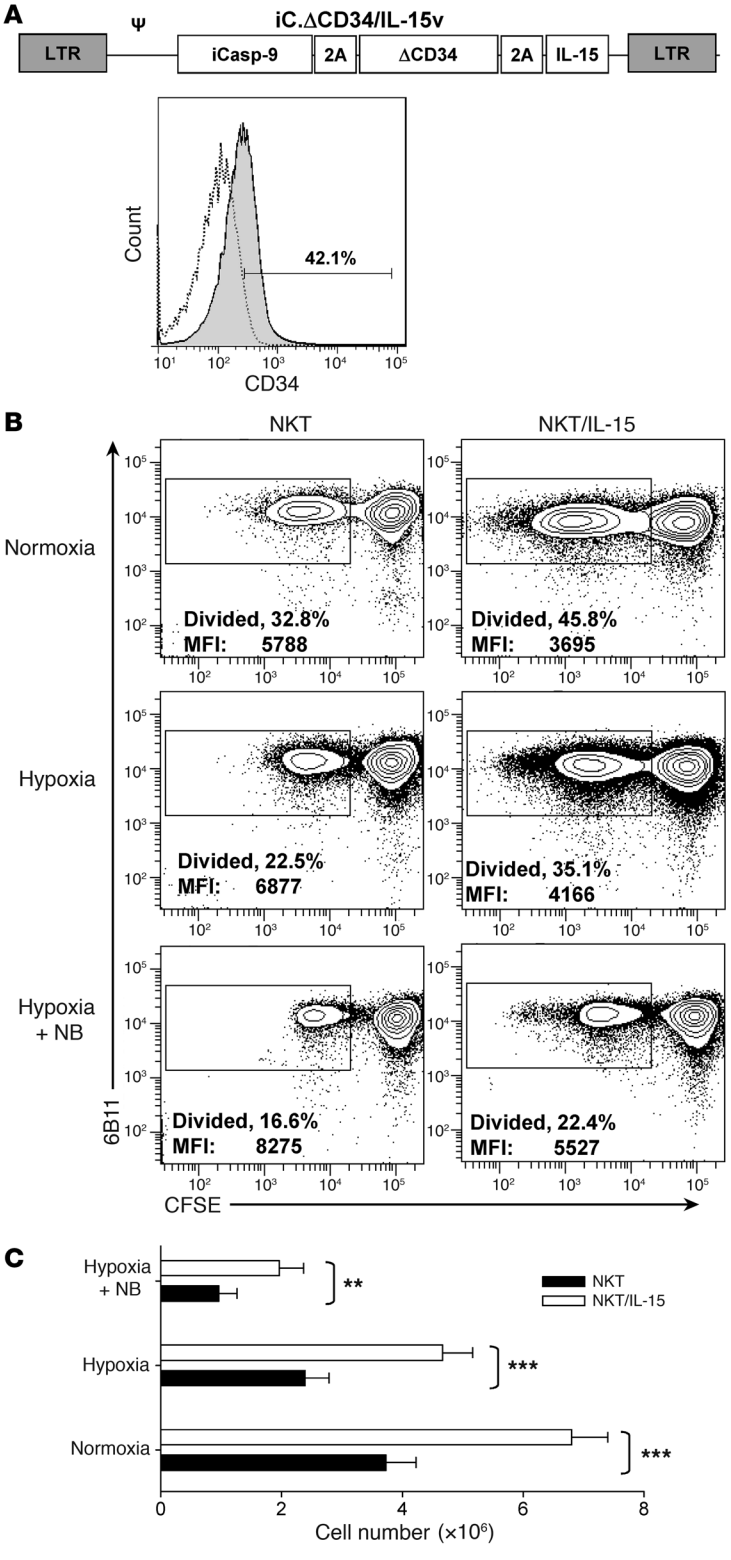

Figure 6

Transgenic expression of IL-15 in NKT cells protects them from hypoxia. (**A**) Retroviral construct used to transduce NKT cells. Proliferating NKT cells were transduced with the IL-15–containing retroviral vector (see Methods), and the transduced cells were identified by FACS using ΔCD34 tag. (**B**) NKT and NKT/IL-15 cells were labeled with CFSE and TCR-stimulated with OKT3 mAb in the absence or presence of NB cells (1:1 ratio) in normoxia or hypoxia (10^6 cells/well). The percent of proliferated cells (loss of CFSE expression) was quantified by FACS after 5-day culture with IL-2 (50 U/ml). Data are from a representative of 4 experiments with NKT cells from 4 donors. (**C**) Absolute number of viable NKT cells was quantified after 5-day culture using hemocytometer and trypan blue staining. Shown are mean ± SD of cells per condition from 4 experiments. $^{**}P < 0.01$; $^{***}P < 0.001$.

trast to normal liver tissues in tumor-free hu-NSG mice, in which no staining for hypoxia was detected (data not shown), metastatic tissues contained both normoxic and hypoxic areas, and more than 90% of NKT cells and myelomonocytic cells were found in the latter (Figure 4A). Quantitative analysis demonstrated that the frequency of NKT cells per 1,000 cells was 14.8% ± 6.3% in hypoxic versus 1.3% ± 1.6% in normoxic areas, and $CD11b^+$ cell frequency was 20.8% ± 8.9% versus 1.1% ± 1.2% ($P < 0.001$ for both; Figure 4B). Therefore, NKT cells colocalize with TAMs in the hypoxic tumor tissues.

NKT cells are inhibited by contact with NB cells and hypoxia. Since NKT cell–mediated killing or inhibition of TAMs is important for their antitumor activity against $CD1d^-$ tumors (12), we asked how the hypoxic tumor environment that is at least in part responsible for NKT cell trafficking toward TAMs affects their viability and function. NKT cells expanded from PBMCs of 4 donors using antigenic stimulation with α-galactosylceramide (αGalCer) were cultured in normoxic and hypoxic conditions for 24 hours, and NKT cell viability was examined by trypan blue exclusion at different time intervals. We found that in the absence of exogenous cytokines, the number of viable NKT cells in hypoxia was only half of that in normoxia. IL-2 and other cytokines that shared common γ chain (IL-15, IL-4, IL-7), with the exception of IL-21, significantly improved NKT cell survival in hypoxia ($P < 0.01$; Figure 5A). While both IL-2 and IL-15 significantly reduced the rate of NKT cell apoptosis in normoxia, neither cytokine significantly protected NKT cells from apoptosis in hypoxia conditions ($P < 0.05$), as measured by annexin V/7-AAD staining (Supplemental Figure 5 and data not shown), which suggests that the observed effect on the absolute number of viable cells was mostly due to cytokine-supported NKT cell proliferation — as we also showed for IL-15–transduced NKT cells (see below) — and is consistent with the metabolic switch of prolifereating lymphocytes to glycolysis with reduced dependence on oxygen (32–35).

To examine the effect of hypoxia on the functional activity of NKT cells, we activated NKT cell TCR by adding agonistic 6B11 mAb and measured cytokine production in cell supernatants by ELISA. After 24 hours of exposure to hypoxia, IFN-γ production by NKT cells cultured alone or with NB cells fell to 31.9% ± 6.1% and 25.7% ± 2.7%, respectively, of that produced in normoxia ($P < 0.001$; Figure 5B). To examine the potential of IL-2Rγ family cytokines to protect NKT cell function from hypoxia, we added saturating concentrations of these cytokines to NKT cell cultures. IL-2 and IL-15, but not other

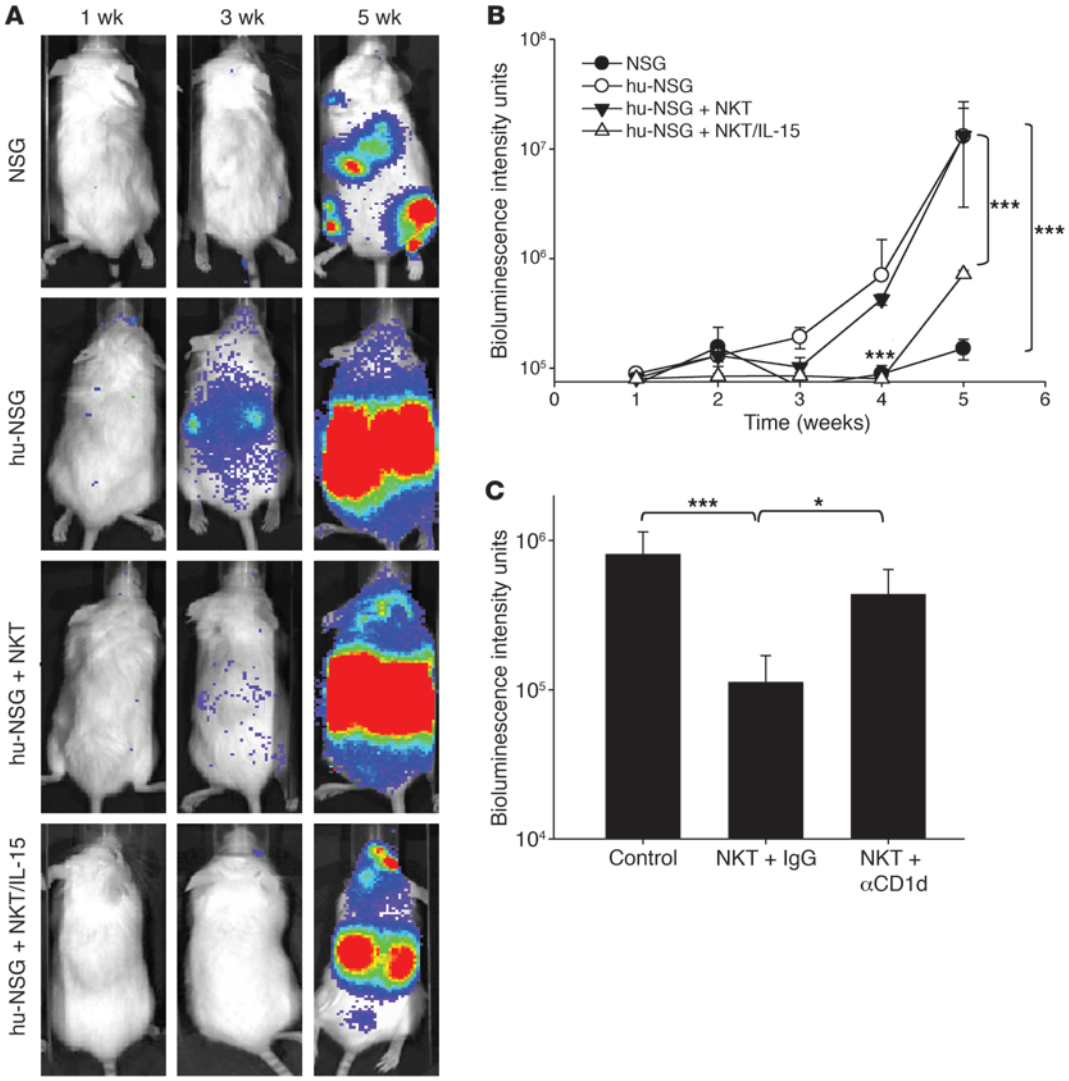

Figure 7

NKT/IL-15 cells have potent antitumor activity in a metastatic NB model in hu-NSG mice. At 3 months after SCT, hu-NSG or control NSG mice received i.v. injection of 10^6 CHLA-255/luc NB cells alone or followed by 10^7 NKT or NKT/IL-15 cells. Metastatic tumor growth was monitored by weekly bioluminescence imaging. (**A**) Representative bioluminescent images at the indicated times after tumor cell injection. (**B**) Mean ± SD values from of 1 of 2 experiments with 5 mice per group. ***$P < 0.001$. (**C**) Mice were pretreated with anti-CD1d blocking or isotype control mAb before transfer of NKT/IL-15 cells. Shown are mean ± SD values at week 5 from of 1 of 2 experiments with 5 mice per group. *$P < 0.05$; ***$P < 0.001$.

cytokines, rescued the IFN-γ response of NKT cells to TCR stimulation in the presence and absence of NB cells ($P < 0.001$; Figure 5B). Therefore, CCL20-mediated chemoattraction of NKT cells toward hypoxic TAMs may lead to the inhibition of NKT cell functional activity that could be reversed by IL-2 or IL-15.

Several recent reports demonstrated that NKT cells play a key role in liver and kidney ischemia-reperfusion injury (36, 37) and in the genesis of the vaso-occlusive crisis in sickle cell disease (38–40). The acute ischemia and inflammation in these conditions have been associated with spontaneous IFN-γ production by NKT cells both in mice and in humans. However, the direct effect of hypoxia on IFN-γ expression in NKT cells has not been evaluated. To examine the effect of hypoxia on spontaneous cytokine production by human NKT cells, we cultured quiescent NKT cells from 4 donors under normoxic or hypoxic conditions for different time intervals (2, 4, 6, 12, 24, and 48 hours) and measured IFN-γ and IL-4 production by ELISA. In the absence of antigenic stimulation, cytokines remained undetectable either in normoxia or hypoxia at all times examined (data not shown), which suggests that hypoxia does not directly stimulate human NKT cells.

IL-15 protects NKT cells and restores their antitumor potential. Our group and others have demonstrated that IL-15 plays a critical role in NKT cell development and homeostatic maintenance (41–43). The results of the present study (Figure 5B) suggest that IL-15 can also protect NKT cells from the inhibitory effect of the hypoxic tumor microenvironment. Therefore, we hypothesized that transgenic expression of IL-15 in adoptively transferred NKT cells would enhance their antitumor potential as a result of improved in vivo persistence and functionality at the tumor site. To test this hypothesis, we transduced NKT cells with a previously described

retroviral construct, containing cDNA of human IL-15, inducible caspase-9 suicide gene (iCasp-9), and CD34 tag (44), to create transgenic IL-15–expressing NKT cells (referred to herein as NKT/IL-15 cells). Ex vivo–expanded human NKT cells were stably transduced with the IL-15–containing vector (Figure 6A). We also confirmed IL-15 production by the transduced NKT cells by ELISA (data not shown). To examine the protective potential of transgenic IL-15 on NKT cell function under hypoxia and in the presence of tumor cells, we used in vitro settings similar to those described for Figure 4B and measured TCR-induced NKT cell proliferation using CFSE dilution assay and apoptosis rate using annexin V staining. Consistent with the observed protective properties of the exogenous recombinant human IL-15, we found that NKT cells/IL-15 had a significantly higher rate of proliferation upon hypoxia alone and in the presence of NB cells than did parental NKT cells ($P < 0.01$; Figure 6B). The antiapoptotic effect of transgenic IL-15 was significant only in normoxic conditions (data not shown), as was the antiapoptotic effect of exogenous IL-15 (Supplemental Figure 5). The absolute cell count at the end of 5-day culture conclusively demonstrated that NKT/IL-15 cells expanded significantly better than did NKT cells in all tested conditions (Figure 6C). Therefore, NKT/IL-15 cells will likely be protected upon antigen recognition in the hypoxic tumor microenvironment.

NKT/IL-15 cells have potent antitumor activity in a metastatic NB model in hu-NSG mice. To examine whether NKT/IL-15 cells have a therapeutic advantage, we used a metastatic NB model in hu-NSG mice. At 3.5 months after SCT and upon confirmation of human hematopoietic reconstitution (Supplemental Figure 4, B and C), mice were i.v. injected with luciferase-transduced human NB cells (CHLA-255/luc). The therapeutic groups also received a single injection of either NKT cells or NKT/IL-15 cells. NSG mice (which did not receive human $CD34^+$ stem cells) were used as a control group to assess the overall effect of human hematopoietic cells on the tumor growth. Metastatic growth in hu-NSG mice was dramatically enhanced compared with NSG mice ($P < 0.001$; Figure 7, A and B), providing further support for the prominent role of BM-derived cells in enhancing NB growth. Whereas immunotherapy with NKT cells had a significant ($P < 0.05$), but short-lived, inhibitory effect on metastatic growth, a single injection of NKT/IL-15 cells completely abrogated the tumor-promoting effect of the human hematopoietic environment ($P < 0.001$ at weeks 4 and 5; Figure 7, A and B). To determine whether the enhanced antitumor activity of NKT/IL-15 cells remains CD1d restricted, we repeated the treatment of NB metastases in hu-NSG mice with NKT/IL-15 cells after pretreatment with anti-CD1d blocking or isotype control mAb. Antitumor efficacy of NKT/IL-15 cells was inhibited by anti-CD1d mAb ($P < 0.05$; Figure 7C), which indicates that the effect of IL-15 depends, at least in part, on the function of CD1d-restricted NKT cells. However, due to incomplete inhibition, a contribution of NKT-independent effects of IL-15, such as activation of NK cells, cannot be excluded. These data suggest that immunotherapy with NKT/IL-15 cells may be effective in patients with metastatic NB and other types of cancer. For the maximum therapeutic benefit, this form of immunotherapy targeting tumor-supportive stroma could be combined with other forms of immunotherapy or chemotherapy that target tumor cells directly.

Discussion

Our present study reveals what we believe to be a novel mechanism of tumor escape from immune control by NKT cells and provides mechanistic insight into the development of NKT cell–based cancer immunotherapy. Because NKT cell antitumor activity against $CD1d^-$ tumors depends on their documented ability to colocalize and interact with $CD1d^+$ TAMs (12), elucidation of the mechanism by which NKT cells traffic toward TAMs and understanding of this process's effect on NKT cell function are critically important for the rational design of NKT cell–based immunotherapy. We show that, besides the previously described requirement for NB cell–derived CCL2 (8), NKT cell migration to the tumor site depended on CCL20, which was produced by TAMs inside the tumor tissues. CCL20 expression was induced in monocytic cells upon contact with NB cells and it was at least partly dependent on mbTNF-α, which was expressed on the surface of NB cells. Moreover, NB cell–induced CCL20 expression in monocytic cells was greatly amplified by hypoxia, which is known to attract TAMs (13, 19, 20). This suggests that the CCL20 gradient directs NKT cell trafficking toward hypoxic tumor tissues. Indeed, we found that more than 90% of tumor-infiltrating NKT cells were colocalized with macrophages in hypoxic areas of NB xenografts in hu-NSG mice. Hypoxia, in turn, inhibited the ability of NKT cells to respond to an antigenic stimulation, which explains how growing tumors can neutralize NKT cell function and rescue tumor-supportive TAMs from NKT cell attack. Importantly, we found that IL-15 protected antigen-activated NKT cells from hypoxia, and NKT/IL-15 cells had potent and long-lasting antitumor activity in a hu-NSG model of metastatic NB.

We found that TAMs in primary NB tumors produced CCL20, expression of which was selectively induced in monocytic cells upon direct contact with NB cells and enhanced by hypoxia. Our quest for the initiating inflammatory signal that triggers induction of CCL20 expression in monocytes upon their contact with tumor cells revealed expression of mbTNF-α on the cell surface in all tested NB cell lines regardless of their MYCN status and the existence of a $mbTNF\text{-}\alpha^+$ NB cell subset, which we believe to be previously unknown, in primary tumors. We demonstrated that NB cells had potent proinflammatory properties, TNF-α–dependently activating the NF-κB signaling pathway in monocytic cells that resulted not only in CCL20 expression, but also in the activation of a defined gene expression program, which is known to be a hallmark of tumor-promoting chronic inflammation (45, 46). For example, NF-κB activated gene expression of IL-6 — a known growth factor for non–MYCN-amplified NB cells — in monocytic cells, and the level of IL-6 mRNA expression negatively correlates with long-term disease-free survival in high-risk NB patients (12). The tumor-promoting role of the TNF-α/NF-κB axis is well-described in epithelial tumors both in mouse models of cancer and in cancer patients (21, 46–48). These are common tumors in adults that can often be etiologically or pathogenetically linked to preexisting chronic inflammatory conditions, such as hepatitis (45) or colitis (46). In contrast, NB as well as other pediatric tumors arises during embryogenesis or early postnatal development in the absence of preexisting chronic inflammation (49). The identification of a subset of NB cells in primary tumors that express mbTNF-α suggests that these cells may initiate tumor-supportive inflammation and could be targeted for therapy with TNF-α antagonists, which are currently being tested in clinical trials in adults with epithelial cancers and hematologic malignancies (50–52). However, incomplete inhibition of CCL20 production in the coculture of monocytes with NB cells by anti–TNF-α mAb suggests that other as-yet unidentified tumor-derived signals may contribute to macrophage activation in NB.

We observed a differential requirement for CCL2 and CCL20 for NKT cell in vitro migration toward a coculture of NB cells with monocytes in normoxic and hypoxic conditions. Whereas CCL2 was required for NKT cell migration in normoxia, CCL20 was largely responsible for their migration in hypoxia. The observed downregulation of CCL2 expression in NB cells under hypoxia combined with CCL20 induction in hypoxic monocytes suggests a 2-step mode of NKT cell migration in the tumor tissues: CCR2- or CCR4-mediated exit from circulation toward CCL2-producing NB cells in the oxygenated areas around blood vessels, and then CCR6-mediated trafficking toward CCL20-producing TAMs in the hypoxic areas. The in vivo blocking experiments with anti-CCL20 neutralizing mAb further support the importance of CCL20 for NKT cell localization to the tumor site. Furthermore, visualization of hypoxic areas within tumor xenografts using intravital staining with EF5 revealed that the vast majority of adoptively transferred NKT cells colocalized with TAMs in the hypoxic areas of the tumor tissues. Therefore, NKT cells may colocalize with TAMs as a component of a novel innate response to tumor-induced hypoxia. Moreover, this mechanism could reflect an evolutionary conserved role of NKT cells in linking tissue hypoxia with inflammation. This concept is supported by several recent reports demonstrating that NKT cells play a key role in the inflammatory response in liver and kidney ischemia-reperfusion injury (36, 37) and in the genesis of the vaso-occlusive crisis in sickle cell disease (38–40). Both in mice with experimental ischemia-reperfusion injury and in humans with sickle cell disease, NKT cells have increased IFN-γ production. However, to our knowledge, the direct effect of hypoxia on NKT cell IFN-γ expression had not previously been examined. We found that hypoxia did not have a direct stimulatory effect on human NKT cells, which suggests that increased IFN-γ production by NKT cells in patients with sickle cell disease could be due to a combined action of hypoxia and inflammatory mediators, in which hypoxia directs NKT cell localization to the site of inflammation rather than directly activating these cells. The ability of NKT cells to recognize and respond to hypoxia could be essential for their control of TAMs at the early stages of tumor progression, when TAMs play a major role in tumor vascularization and tumor cell survival (13–15, 53). However, growing tumor may also use the same phenomenon for the immune escape by trapping NKT cells in the hypoxic tissues and disabling their function.

We found that NKT cell viability and function were affected by hypoxia and that antigen-dependent proliferation and cytokine production was protected by IL-2 or IL-15. The protective effect of these cytokines on proliferating rather than quiescent NKT cells was consistent with similar observations in T cells, which have previously been shown to switch to glycolysis upon antigenic stimulation and to require less oxygen (34, 35). Studies in mice have demonstrated that NKT cell development, homeostatic maintenance, and survival largely depend on IL-15 (42, 43). Our group previously reported that IL-15 also stimulates proliferation and enhances survival of human NKT cells (41). Human $CD4^-$ NKT cells, which are mostly $CD8^-CD4^-$ double-negative (DN), express much higher levels of IL-2Rβ than do $CD4^+$ cells, so that IL-15 preferentially expands DN NKT cells (41). Importantly, DN NKT cells are more cytotoxic than are $CD4^+$ NKT cells, and a recent report demonstrated that only DN NKT cells are required for antitumor responses in vivo (54). This suggests that the expression of IL-15 in NKT cells for therapeutic purposes would support expansion, persistence, and antitumor activity of DN NKT cells in cancer patients. We indeed found that transduction of NKT cells with IL-15 cDNA protected them from the inhibitory effects of NB cells and hypoxia. Importantly, NKT/IL-15 cells demonstrated a potent therapeutic activity against NB metastases in hu-NSG mice, and this effect was at least in part CD1d dependent. Besides acting directly on NKT cells and enhancing their activity against TAMs, locally produced IL-15 is expected to activate other antitumor immune effector cells, such as NK and tumor-specific $CD8^+$ T cells (55). In contrast to IL-2, IL-15 does not fully activate Tregs (56), which are known to have an inhibitory effect on NKT cells (57) and could counteract their antitumor activity. To ensure the safety of the potential clinical use of NKT/IL-15 cells, we incorporated a suicide gene, iCasp-9, which allows the elimination of transgeneic cells upon its pharmacologic activation with a nontoxic small molecular drug, AP20187 (58–60). We previously demonstrated that T cells expressing the iCasp-9 molecule are efficiently eliminated upon pharmacologic activation of the suicide gene both in vitro and in vivo (59, 60), not only in a mouse model, but also in lymphoma patients (61). Therefore, NKT/IL-15 cell therapy under iCasp-9 control is expected to be safe and needs to be tested in patients with recurrent/resistant NB.

In summary, we have identified the mechanism by which NKT cells are attracted toward TAMs in tumor tissues. This mechanism could reflect a broader role of NKT cells in the regulation of inflammation and will need to be further investigated, not only in the context of tumor-associated inflammation, but also in chronic infectious and autoimmune diseases. The enabling NKT cell tumor localization and functional activity at the tumor site via pharmacological modulation or/and genetic engineering of NKT cells, as demonstrated herein, may lead to the development of effective and broadly applicable cancer immunotherapies.

Methods

Human specimens. 7 primary NB specimens were obtained from surgery of biopsy at diagnosis at Texas Childrens Cancer Center, Baylor College of Medicine. For FACS analysis, tissues were homogenized and digested with dispase II (Roche), collagenase (Sigma-Aldrich), and DNase I into single cell suspensions. The remaining tissues were embedded in OCT and maintained at –80°C. Cord blood was obtained from a cord blood bank at the MD Anderson Cancer Center.

Cell lines. CHLA-15, CHLA-255, CHLA-255/luc, LA-N-1, SK-N-BE(2), CHLA-90, and IMR32 NB cell lines were established and maintained as previously described (8, 25, 62). 293T cells were purchased from ATCC and maintained in IMDM plus 10% FBS (Hyclone) and 2 mM GlutaMAX-I (Gibco-BRL, Invitrogen).

Plasmids and retrovirus production. 2 SFG retroviral vectors, SFG.iCasp-9.2A.ΔCD34.2A.IL-15 and SFG.eGFP.FFluc, were constructed as previously described (44) and used to transduce NKT cells. To produce retroviral supernatants, 293T cells were cotransfected with 3 plasmids (Peg-Pam-e encoding for gag-pol, DRF encoding for the RDF114 viral envelope, and the retroviral construct) using the Genejuice transfection reagent (Merck KGaA), and viral supernatants were collected 48 and 72 hours later.

RNA isolation and real-time RT-PCR. Total RNA from cell pellets was isolated using TRIzol (Invitrogen). The RNA quality was assessed with gel electrophoresis prior to reverse transcription into cDNA using M-MLV reverse transcriptase with oligo dT priming (Invitrogen). qRT-PCR was performed with iQ Sybr green supermix assay using the iCycler iQ multicolor real-time PCR detection system (Bio-Rad). Primers were ordered from Sigma (Supplemental Table 1). The relative change in gene expression was

calculated based on the ΔCt method using housekeeping gene lysosomal-associated transmembrane protein 5 (*LAPTM5*) as the control.

NKT cell expansion, culture, and transduction. NKT cell lines were expanded from PBMCs of healthy volunteers as previously described (8), with modifications. Briefly, PBMCs were isolated by buffy coats by Ficoll-Hypaque gradient density centrifugation. NKT cells were purified by anti-iNKT microbeads (Miltenyi Biotec). The negative PBMC fraction was irradiated (150 Gy) and aliquoted. NKT cells were stimulated with an aliquot of autologous PBMCs pulsed with αGalCer (100 ng/ml; Funakoshi Co.). rhIL-2 (50 U/ml, BDP, NCI-Frederick) was added at the second day and then every other day. NKT cells were restimulated every 2 weeks with the remaining PBMC aliquots. The phenotype and purity of NKT cells were assessed using mAbs for CD3, Vα24-Jα18 (6B11), and CD4. Proliferating NKT cells were transduced with retroviral supernatants on day 5 after restimulation in non–culture-treated 24-well plates precoated with recombinant fibronectin fragment (FN CH-296; Retronectin, Takara Shuzo). The rate of NKT cell transduction was measured by FACS with anti-CD34–PE mAb. The transduced NKT cells then continued expansion in the presence of rhIL-2.

Expanded NKT cells (7 days after restimulation) were cultured under normoxic (20% O_2) or hypoxic (1% O_2 in a Hearcell 240i tri-gas incubator; Thermo Scientific) conditions for 24 or 48 hours in the absence or presence of one of the following cytokines: rhIL-2 (NIH), IL-15, IL-4, IL-7 (10 ng/ml each; Peprotech), or IL-21 (eBiosciences) at 200 U/ml each. The absolute number of viable cells was quantified using the trypan blue exclusion method.

Monocyte isolation and coculture experiments. PBMCs were isolated by gradient centrifugation from buffy coats purchased from Gulf Cost Regional Blood Center. Monocytes were isolated by negative selection using Monocyte Isolation kit II (Miltenyi Biotec) according to the manufacturer's instructions. In coculture experiments, monocytes were added directly to NB cells or to the inserts separated by 0.4 μm membrane (Costar Corning) from NB cells. Where indicated, NB cells were preincubated with anti-human TNF-α neutralizing antibody (clone 1825; R&D Systems) or isotype control IgG1 (clone 11711; R&D Systems) for 1 hour before coculture with monocytes. We then cultured cells under hypoxic (1% O_2) or normoxic (20% O_2) conditions and collected supernatants at the indicated time points.

Multiplex cytokine quantification assay and ELISA. Cytokines released by NKT cells were assessed by CBAPlex beads (BD Biosciences) on FACS-Array analyzer according to the manufacture's manual and as previously described (8). CCL20 level in the coculture supernatants was determined using human CCL20/MIP-3 alpha Quantikine ELISA Kit (R&D Systems).

In vitro migration assay. NKT cell in vitro migration was assessed using permeable Transwell inserts (5 μm; Corning Costar). Where indicated, supernatants from monocyte and NB cells in bottom chambers were preincubated with isotype control (clone 11711) or neutralizing antibody against CCL20 (clone 67310) or CCL2 (clone 24822) (R&D Systems) for 1 hour before adding NKT cells in the upper chambers. Quantitative analysis of NKT cell migration was performed by FACS, as previous described (25).

Flow cytometry (FACS). To analyze the expression of CCL20 in monocytes, cells were first incubated with GolgiStop (BD Biosciences) for 4 hours and then stained with the following surface markers: CD56-APC, CD14-APC.Cy7, CD33-PE.Cy7, and CD45-PerCP (BD Biosciences). Cells were then fixed and permebalized with a Perm/Fix Kit (BD Biosciences) and intracellularly stained with CCL20-PE (BD Biosciences). To determine the level of CCR6 expression on NKT cells, cells were surface stained with CD3-APC, 6B11-FITC, CD4-PE.Cy7, and CCR6-PE (BD Biosciences).

To monitor the development of human hematopoiesis in hu-NSG mice, the following set of antibodies was used: anti-human CD45-FITC, anti-mouse CD45-PerCP, CD14-PE, CD33-PE.Cy7, CD3-APC (BD Biosciences), and CD20-APC.Cy7 (Biolegend). The antibody set CD45-PerCP, CD3-APC, and CD34-PE (BD Biosciences) was used to assess purity of the human $CD34^+$ stem cells. The antibodies CD45-PerCP, CD3-APC, 6B11-FITC, CD14-APC.Cy7, HLADR-PE.Cy7, and CD1d-PE (all BD Biosciences) were used to identify tumor-infiltrating leukocytes in human primary NB tumor and tumor xenografts from hu-NSG mice. Additionally, primary NBs were analyzed for NB surface marker expression using the antibodies CD45-PerCP, CD56-APC (BD Biosciences), and TNF-α–FITC (clone 6401; R&D Systems).

To determine NKT cell proliferation, cells were first labeled with CFSE (Invitrogen) and then restimulated by anti-TCR agonistic mAb (6B11 or OKT3) followed by a 5-day culture with or without NB cells under hypoxic or normoxic conditions. Cells were then surface stained with 6B11-PE and CD3-APC mAbs and analyzed by flow cytometry to determine CFSE dilution in $CD3^+6B11^+$ cells.

The expression levels of IκBα and phosphorylated NF-κB p65 were determined by FACS in monocytes according to the manufacturer's protocols (BD PhosFlow). Briefly, $1–2 \times 10^6$ ml^{-1} monocytes were cultured with or without CHLA-255 NB cell line (~70%–80% confluence) in the presence of neutralizing anti–TNF-α or suitable isotype control for the indicated times. After incubation, cells were fixed immediately by adding an equal volume of prewarmed to 37C BD PhosFlow Cytofix fixation buffer; plates were incubated for an additional 10 minutes at 37°C, and then the cells were harvested. For permeabilization, BD Phosflow Perm Buffer IV, precooled at –20°C, was added drop by drop to the cell pellet and incubated for an additional 15–20 minutes at room temperature. The tubes were stored at –20°C until stained with Alexa Fluor 488 phosphospecific anti–NF-κB p65 mAb (or PE-labeled IκBα) and PE- or APC-labeled anti-CD56 mAb to identify NBs and monocytes in coculture. Analysis was performed on a LSR-II 4-laser flow cytometer (BD Biosciences) using BD FACDiva software version 6.0 and FlowJo 7.2.5 (Tree Star Inc.).

4-color immunofluorescent microscopy. Mouse livers were removed and cut into workable sizes. The tissues were then frozen in OCT and kept at –80°C until use. 10-μm frozen sections were made using Cryostat (HM550; Thermo Scientific) and immediately fixed in 4% paraformaldehyde for 1 hour at room temperature. The fixed sections were treated twice with 0.1% sodium borohydrite for 5 minutes and then rinsed 3 times in PBS containing 0.013% sodium azide and 0.004% thimerosal. Slides were blocked with 5% normal mouse serum plus 1.5% BSA and 0.3% skim milk in ttPBS (PBS containing 0.3% Tween 20, 0.013% azide, and 0.004% thimerosal) for 1 hour at room temperature. After blocking, tissue sections were incubated with mouse anti-human CD11b (Mac-1) antibody (PN IM0190; Beckman Coulter) diluted at 1:400 in ttPBS supplemented with 1.5% BSA at 4°C overnight. The tissue sections were then washed twice with ttPBS and once with 1× PBS, 15 minutes each time. The fluorescent Alexa Fluor 647–conjugated goat anti-mouse secondary antibody (A31517, 1:800; Invitrogen) was incubated with the sections for 1 hour at room temperature and rinsed 3 times as described above. The slides were refixed in 4% paraformaldehyde for 25 minutes and blocked again for 1 hour at room temperature before proceeding to the next step. The above-stained slides were incubated with Cy3-conjugated anti-EF5 antibody (ELK-351; Hypoxia-Imaging, Department of Radiation Oncology, University of Pennsylvania) overnight at 4°C, followed by 2 rinses in ttPBS and 1 rinse in 1× PBS, 45 minutes each time. The slides were then counterstained with ProLong Gold antifade reagent (P36930; Invitrogen) and coverslipped. The 4-color fluorescent images of the stained sections were acquired on a Nikon A1-Rs inverted Laser Scanning (Confocal) Microscope. For the quantification of CFSE-labeled NKT cells and Alexa Fluor–labeled CD11b cells in either normoxic or hypoxic regions, all the images were captured using the same setting, i.e., at the same PMT HV for each channel. The images were analyzed by Annotation and Measurement feature of the NIS Elements AR3.2 software. In each imaged region, the expression of EF5 was quantified as the intensity of Cy3

(shown as red), and the absolute numbers of NKT cells (shown as green) and the CD11b$^+$ cells (shown as purple) were counted. The regions for which the mean intensity of Cy3 was lower than 200 were defined as normoxia, whereas those areas for which the mean intensity of Cy3 was at least 2-fold higher were defined as hypoxia. 10 images from either normoxic or hypoxic regions were compared.

In vivo experiments. NOD/SCID/IL-2Rγ–null (NSG) mice were bred in the Texas Children's Hospital animal facility. 4-week-old mice were irradiated with 225 cGy and injected with human cord blood–derived CD34$^+$ stem cells, as previously described (26, 27), to generate hu-NSG mice. The frequency of CD34$^+$ cells was >95%, and the contamination by CD3$^+$ cells was <0.1% in the stem cell transplants. 3 months after SCT, reconstitution of human hematopoiesis was confirmed in peripheral blood by FACS, and mice were i.v. injected with human CHLA-255/luc cells, either under the renal capsule (localization experiments), as previously described (63), or i.v. (therapeutic experiments). Tumor growth was indirectly assessed by weekly bioluminescent imaging (Small Animal Imaging Core facility, Texas Children's Hospital). Where indicated, mice were injected i.p. with 100 μg/mouse of neutralizing anti-CCL2 (clone 24822), anti-CCL20 (clone 67310), both, or isotype control (clone 11711) mAb (R&D Systems). Some animals received i.v. injections of ex vivo–expanded human NKT cells (1–5 × 10^7 cells). Before injection into animals, NKT cells had been cultured with IL-2 (50 U/ml; Peprotech) for 7–10 days without TCR stimulation to achieve resting phase, when their trafficking pattern more closely resembled that of primary NKT cells, as we determined previously (8). When indicated, mice received i.p. injection of anti-hCD1d blocking mAb, 42.1 or isotype control (50 μg/ml; BD Biosciences). Mice were euthanized, and cell suspensions prepared from tumors were analyzed by multicolor flow cytometry as described in *Flow cytometry (FACS)*. When indicated, NKT cell antitumor efficacy was determined by bioluminescent imaging. To determine NKT cell distribution in normoxic versus hypoxic tumor tissues, NKT cells were labeled with CellTrace CFSE cell proliferation kit according to the manufacturer's protocol (Invitrogen) before injection. For labeling hypoxic tissues, mice were i.v. injected with 250 μl EF5 (100 mM solution, produced at NCI at no cost and provided by C.J. Koch, University of Pennsylvania, Philadelphia, Pennsylvania, USA). After 3 hours, mice were euthanized, and parts of their tumors were excised and immediately embedded in OCT medium to be used for immunofluorescent staining of EF5, NKT, and TAMs.

Statistics. Statistical analysis was performed using GraphPad Prism 5.0 software (GraphPad). Comparisons between groups were based on 1- or 2-way ANOVA, depending on whether 1 (e.g., CCL20 concentration) or 2 (e.g., CCL20 concentration in normoxic and hypoxic conditions) independent variables were measured. We also used the Bonferroni post-test to compare selected experimental groups according to the experimental design. All statistical tests were 2-sided, and a P value less than 0.05 was considered statistically significant.

Study approval. Primary NBs specimens were used in accordance with Baylor College of Medicine IRB-approved protocols H-26691 and H-6650. Cord blood was used in accordance with MD Anderson Cancer Center IRB-approved protocol H-20911. Informed consent was obtained in accordance with institutional review board policies and procedures for research dealing with human specimens. Animal experiments were performed according to IACUC-approved protocols at Baylor College of Medicine.

Acknowledgments

We thank Malcolm Brenner (Center for Cell and Gene Therapy, BCM, Houston, Texas, USA) for helpful discussions and James Broughman (Integrated Microscopy Core, Department of Molecular and Cellular Biology, BCM, Houston, Texas, USA) for excellent technical assistance. This work was supported by NIH grants (2RO1 CA116548 to L.S. Metelitsa; R01 CA142636 to G. Dotti), U.S. Department of Defense (W81XWH-10-10425 to G. Dotti), Cancer Prevention and Research Institute of Texas grants (RP1 100528 and RP1 110129 to L.S. Metelitsa), and The Caroline Wiess Law Scholar Award (to L.S. Metelitsa).

Received for publication June 17, 2011, and accepted in revised form March 21, 2012.

Address correspondence to: Leonid S. Metelitsa, Department of Pediatrics, Baylor College of Medicine, 1102 Bates Ave., C.1760.06, Houston, Texas 77030, USA. Phone: 832.824.4395; Fax: 832.825.4846; E-mail: lsmeteli@txch.org.

1. Kronenberg M, Gapin L. The unconventional lifestyle of NKT cells. *Nat Rev Immunol*. 2002;2(8):557–568.
2. Swann J, Crowe NY, Hayakawa Y, Godfrey DI, Smyth MJ. Regulation of antitumour immunity by CD1d-restricted NKT cells. *Immunol Cell Biol*. 2004; 82(3):323–331.
3. Swann JB, Coquet JM, Smyth MJ, Godfrey DI. CD1-restricted T cells and tumor immunity. *Curr Top Microbiol Immunol*. 2007;314:293–323.
4. Berzofsky JA, Terabe M. The contrasting roles of NKT cells in tumor immunity. *Curr Mol Med*. 2009; 9(6):667–672.
5. Yanagisawa K, Seino K, Ishikawa Y, Nozue M, Todoroki T, Fukao K. Impaired proliferative response of V alpha 24 NKT cells from cancer patients against alpha-galactosylceramide. *J Immunol*. 2002; 168(12):6494–6499.
6. Tahir SM, et al. Loss of IFN-gamma production by invariant NK T cells in advanced cancer. *J Immunol*. 2001;167(7):4046–4050.
7. Dhodapkar MV, et al. A reversible defect in natural killer T cell function characterizes the progression of premalignant to malignant multiple myeloma. *J Exp Med*. 2003;197(12):1667–1676.
8. Metelitsa LS, et al. Natural killer T cells infiltrate neuroblastomas expressing the chemokine CCL2. *J Exp Med*. 2004;199(9):1213–1221.
9. Tachibana T, et al. Increased intratumor Valpha24-positive natural killer T cells: a prognostic factor for primary colorectal carcinomas. *Clin Cancer Res*. 2005;11(20):7322–7327.
10. Molling JW, et al. Low levels of circulating invariant natural killer T cells predict poor clinical outcome in patients with head and neck squamous cell carcinoma. *J Clin Oncol*. 2007;25(7):862–868.
11. Metelitsa LS, et al. Human NKT cells mediate antitumor cytotoxicity directly by recognizing target cell CD1d with bound ligand or indirectly by producing IL-2 to activate NK cells. *J Immunol*. 2001; 167(6):3114–3122.
12. Song L, et al. Valpha24-invariant NKT cells mediate antitumor activity via killing of tumor-associated macrophages. *J Clin Invest*. 2009;119(6):1524–1536.
13. Mantovani A, Allavena P, Sica A, Balkwill F. Cancer-related inflammation. *Nature*. 2008; 454(7203):436–444.
14. Sica A, et al. Macrophage polarization in tumour progression. *Semin Cancer Biol*. 2008;18(5):349–355.
15. Sica A, Bronte V. Altered macrophage differentiation and immune dysfunction in tumor development. *J Clin Invest*. 2007;117(5):1155–1166.
16. De Santo C, et al. Invariant NKT cells reduce the immunosuppressive activity of influenza A virus-induced myeloid-derived suppressor cells in mice and humans. *J Clin Invest*. 2008;118(12):4036–4048.
17. De Santo C, et al. Invariant NKT cells modulate the suppressive activity of IL-10-secreting neutrophils differentiated with serum amyloid A. *Nat Immunol*. 2010;11(11):1039–1046.
18. O'Konek JJ, et al. Mouse and human iNKT cell agonist beta-mannosylceramide reveals a distinct mechanism of tumor immunity. *J Clin Invest*. 2011; 121(2):683–694.
19. Allavena P, Sica A, Solinas G, Porta C, Mantovani A. The inflammatory micro-environment in tumor progression: the role of tumor-associated macrophages. *Crit Rev Oncol Hematol*. 2008;66(1):1–9.
20. Mantovani A, Schioppa T, Porta C, Allavena P, Sica A. Role of tumor-associated macrophages in tumor progression and invasion. *Cancer Metastasis Rev*. 2006;25(3):315–322.
21. Grivennikov SI, Greten FR, Karin M. Immunity, inflammation, and cancer. *Cell*. 2010;140(6):883–899.
22. Kim CH, Johnston B, Butcher EC. Trafficking machinery of NKT cells: shared and differential chemokine receptor expression among Valpha24(+)Vbeta11(+) NKT cell subsets with distinct cytokine-producing capacity. *Blood*. 2002;100(1):11–16.
23. Kim CH, Butcher EC, Johnston B. Distinct subsets of human Valpha24-invariant NKT cells: cytokine responses and chemokine receptor expression. *Trends Immunol*. 2002;23(11):516–519.
24. Thomas SY, et al. CD1d-restricted NKT cells express a chemokine receptor profile indicative of Th1-type inflammatory homing cells. *J Immunol*. 2003;171(5):2571–2580.
25. Song L, et al. Oncogene MYCN regulates localiza-

tion of NKT cells to the site of disease in neuroblastoma. *J Clin Invest*. 2007;117(9):2702–2712.
26. Yahata T, et al. Functional human T lymphocyte development from cord blood CD34+ cells in nonobese diabetic/Shi-scid, IL-2 receptor gamma null mice. *J Immunol*. 2002;169(1):204–209.
27. Giassi LJ, et al. Expanded CD34+ human umbilical cord blood cells generate multiple lymphohematopoietic lineages in NOD-scid IL2rgamma(null) mice. *Exp Biol Med (Maywood)*. 2008;233(8):997–1012.
28. Battaglia F, et al. Hypoxia transcriptionally induces macrophage-inflammatory protein-3alpha/CCL-20 in primary human mononuclear phagocytes through nuclear factor (NF)-kappaB. *J Leukoc Biol*. 2008;83(3):648–662.
29. Goillot E, et al. Tumor necrosis factor as an autocrine growth factor for neuroblastoma. *Cancer Res*. 1992;52(11):3194–3200.
30. Seeger RC, Atkinson J, Reynolds CP. Neuroblastoma. In: Holland JF, Frei E III, Bast RC Jr, Kufe DW, Morton DL, Weichsenbaum RR, eds. *Cancer Medicine*. Philadelphia, Pennsylvania, USA: Lea and Febiger; 1996:2991–3020.
31. Facciabene A, et al. Tumour hypoxia promotes tolerance and angiogenesis via CCL28 and T(reg) cells. *Nature*. 2011;475(7355):226–230.
32. Roos D, Loos JA. Changes in the carbohydrate metabolism of mitogenically stimulated human peripheral lymphocytes. II. Relative importance of glycolysis and oxidative phosphorylation on phytohaemagglutinin stimulation. *Exp Cell Res*. 1973;77(1):127–135.
33. Krauss S, Brand MD, Buttgereit F. Signaling takes a breath--new quantitative perspectives on bioenergetics and signal transduction. *Immunity*. 2001; 15(4):497–502.
34. Frauwirth KA, et al. The CD28 signaling pathway regulates glucose metabolism. *Immunity*. 2002; 16(6):769–777.
35. Jones RG, Thompson CB. Revving the engine: signal transduction fuels T cell activation. *Immunity*. 2007;27(2):173–178.
36. Lappas CM, Day YJ, Marshall MA, Engelhard VH, Linden J. Adenosine A2A receptor activation reduces hepatic ischemia reperfusion injury by inhibiting CD1d-dependent NKT cell activation. *J Exp Med*. 2006;203(12):2639–2648.
37. Li L, et al. NKT cell activation mediates neutrophil IFN-gamma production and renal ischemia-reperfusion injury. *J Immunol*. 2007;178(9):5899–5911.
38. Wallace KL, et al. NKT cells mediate pulmonary inflammation and dysfunction in murine sickle cell disease through production of IFN-gamma and CXCR3 chemokines. *Blood*. 2009;114(3):667–676.
39. Wallace KL, Linden J. Adenosine A2A receptors induced on iNKT and NK cells reduce pulmonary inflammation and injury in mice with sickle cell disease. *Blood*. 2010;116(23):5010–5020.
40. Field JJ, Nathan DG, Linden J. Targeting iNKT cells for the treatment of sickle cell disease. *Clin Immunol*. 2011;140(2):177–183.
41. Baev DV, et al. Distinct homeostatic requirements of CD4+ and CD4- subsets of Valpha24-invariant natural killer T cells in humans. *Blood*. 2004; 104(13):4150–4156.
42. Matsuda JL, et al. Homeostasis of V alpha 14i NKT cells. *Nat Immunol*. 2002;3(10):966–974.
43. Gordy LE, et al. IL-15 regulates homeostasis and terminal maturation of NKT cells. *J Immunol.* 2011; 187(12):6335–6345.
44. Hsu C, et al. Cytokine-independent growth and clonal expansion of a primary human CD8+ T-cell clone following retroviral transduction with the IL-15 gene. *Blood*. 2007;109(12):5168–5177.
45. Pikarsky E, et al. NF-kappaB functions as a tumour promoter in inflammation-associated cancer. *Nature*. 2004;431(7007):461–466.
46. Greten FR, et al. IKKbeta links inflammation and tumorigenesis in a mouse model of colitis-associated cancer. *Cell*. 2004;118(3):285–296.
47. Szlosarek P, Charles KA, Balkwill FR. Tumour necrosis factor-alpha as a tumour promoter. *Eur J Cancer*. 2006;42(6):745–750.
48. Affara NI, Coussens LM. IKKalpha at the crossroads of inflammation and metastasis. *Cell*. 2007; 129(1):25–26.
49. Maris JM, Hogarty MD, Bagatell R, Cohn SL. Neuroblastoma. *Lancet*. 2007;369(9579):2106–2120.
50. Szlosarek PW, Balkwill FR. Tumour necrosis factor alpha: a potential target for the therapy of solid tumours. *Lancet Oncol*. 2003;4(9):565–573.
51. Brown ER, et al. A clinical study assessing the tolerability and biological effects of infliximab, a TNF-alpha inhibitor, in patients with advanced cancer. *Ann Oncol*. 2008;19(7):1340–1346.
52. Friedberg J, et al. Targeting the follicular lymphoma microenvironment through blockade of TNFalpha with etanercept. *Leuk Lymphoma*. 2008; 49(5):902–909.
53. Pietras A, et al. HIF-2alpha maintains an undifferentiated state in neural crest-like human neuroblastoma tumor-initiating cells. *Proc Natl Acad Sci U S A*. 2009;106(39):16805–16810.
54. Crowe NY, et al. Differential antitumor immunity mediated by NKT cell subsets in vivo. *J Exp Med*. 2005;202(9):1279–1288.
55. Waldmann TA. The biology of interleukin-2 and interleukin-15: implications for cancer therapy and vaccine design. *Nat Rev Immunol*. 2006;6(8):595–601.
56. Wuest TY, Willette-Brown J, Durum SK, Hurwitz AA. The influence of IL-2 family cytokines on activation and function of naturally occurring regulatory T cells. *J Leukoc Biol*. 2008;84(4):973–980.
57. La Cava A, Van Kaer L, Fu DS. CD4+CD25+ Tregs and NKT cells: regulators regulating regulators. *Trends Immunol*. 2006;27(7):322–327.
58. Straathof KC, et al. An inducible caspase 9 safety switch for T-cell therapy. *Blood*. 2005;105(11):4247–4254.
59. Tey SK, Dotti G, Rooney CM, Heslop HE, Brenner MK. Inducible caspase 9 suicide gene to improve the safety of allodepleted T cells after haploidentical stem cell transplantation. *Biol Blood Marrow Transplant*. 2007;13(8):913–924.
60. Quintarelli C, et al. Co-expression of cytokine and suicide genes to enhance the activity and safety of tumor-specific cytotoxic T lymphocytes. *Blood*. 2007;110(8):2793–2802.
61. Di Stasi A, et al. Inducible apoptosis as a safety switch for adoptive cell therapy. *N Engl J Med*. 2011; 365(18):1673–1683.
62. Reynolds CP, et al. Biological classification of cell lines derived from human extra-cranial neural tumors. *Prog Clin Biol Res*. 1988;271:291–306.
63. Kim ES, et al. Potent VEGF blockade causes regression of coopted vessels in a model of neuroblastoma. *Proc Natl Acad Sci U S A*. 2002;99(17):11399–11404.